

An effective single molecule model that simulates dynamics of collective strong light-matter coupling

Juan B. Pérez-Sánchez, Arghadip Koner, Joel Yuen-Zhou

*Department of Chemistry and Biochemistry, University of California San Diego, La Jolla, California, 92093**

Nathaniel P. Stern

Department of Physics and Astronomy, Northwestern University, Evanston, Illinois 60208, United States

(Dated: September 13, 2022)

Molecular polaritons are hybrid light-matter states that emerge when the coupling between molecules and a photon mode exceeds the cavity and molecular decay rates. They have been of much recent interest due to their potential use to control molecular properties and processes. From the theoretical standpoint, the study of molecular polaritons beyond simple quantum emitter ensemble models (e.g., Tavis-Cummings) is challenging due to the large dimensionality of these systems (the number of molecular emitters is $N \approx 10^6 - 10^{10}$), as well as the complex interplay of molecular electronic and nuclear degrees of freedom, which is absent or much reduced in atomic and solid-state polariton systems, respectively. A very important question is the extent to which single molecule models can be used for interpretation or prediction of molecular polaritonic phenomena. In this work, we exploit permutational symmetries to drastically reduce the computational cost of *ab-initio* quantum dynamics simulations for large N . In particular, we find that using an *effective* single-molecule to calculate the dynamics in the collective regime is formally justified when $N \rightarrow \infty$. Based on this result, we discuss how to seamlessly modify existing single-molecule strong coupling calculations to generate these effective models as well as the crucial differences in phenomena predicted by each type of calculation. We also systematically derive finite N corrections to the dynamics, and show that addition of an extra surrogate molecule is enough to account for couplings that scale as $\mathcal{O}(1/\sqrt{N})$. This formalism is benchmarked against well-known results of polariton relaxation rates, and used to develop much needed intuition to generate robust strategies for polariton chemistry, and applied to describe a cavity-assisted energy funneling mechanism between different molecular species.

I. INTRODUCTION

Molecular polaritons are quasiparticles arising when vibrational and/or electronic excitations of an ensemble of molecules are collectively coupled to a confined electromagnetic mode such as those found in optical microcavities. These systems have attracted much interest in the last decade due to their potential applications in altering chemical reactions dynamics [1–6], energy transfer and energy conversion mechanisms [7–13], and as a framework to achieve room-temperature exciton-polariton condensation [14, 15]. Theoretical work aimed at explaining experimental results or predicting new phenomena emerging in polaritonic architectures face the formidable challenge of properly modeling the molecular (local) degrees of freedom of each molecule while describing the super-radiant interaction of the molecular ensemble with the field (collective). The dynamics arising from the complex interplay of vibrational and electronic degrees of freedom in molecules renders simple quantum optics models (such as the original Tavis-Cummings Hamiltonian [16]), limited in their applicability to molecular polaritons. Thus, molecular polaritons face unique challenges and opportunities that are not encountered in more traditional polariton systems with atomic or artificial qubit ensembles [17], or cryogenic inorganic semicon-

ductors [18]. Most of the reported simulations of molecular polaritons can only deal with one of two aforementioned challenges at a time. On the one hand, theoretical studies that acknowledge the collective nature of the light-matter coupling are typically limited to a few dozen molecules at a time and involve sophisticated numerical treatments [19], simplifications such as single-mode treatments [20], or semiclassical trajectories [21]. On the other hand, models that implement *ab initio* treatments are often restricted to a single molecule in a cavity, raising questions about their applicability in the collective strong coupling regime. Regardless, from a computational standpoint, it seems suspicious that it is necessary to explicitly simulate the dynamics of N molecules, especially if they are identical to each other. Indeed, there are numerous symmetries in the system that should significantly reduce the computational cost of these simulations [22–30]. In this work, we outline a wavefunction-based formalism that makes use of such symmetries to significantly reduce the complexity of quantum dynamics simulations of the single-excitation manifold of molecular polaritons. Moreover, this formalism naturally provides a hierarchy or approximations to further simplify the problem in a way that, in the large N limit, it does not scale with the number of molecules in the system for a fixed collective light-matter coupling $\sqrt{N}g$, where g is the single-molecule coupling. In fact, we show how in the $N \rightarrow \infty$ limit, polaritonic properties can be calculated using a modified *effective* single-molecule coupled to a cavity with the collective coupling. This provides

* Email: joelyuen@ucsd.edu

grounds for some single-molecule strong coupling phenomena to appear in the collective regime, consistent with previous work where linear optical properties can be calculated from effective single-molecule models in the thermodynamic limit [31, 32]. The possibility to study disordered ensembles (e.g., a mixture with two chemical species) is discussed. The article is organized as follows: In Section II we present the Hamiltonian and the multi-configurational representation of the total wavefunction of the system, in which permutational symmetries become evident. In Section III we make use of the effective single-molecule model to demonstrate how both optical and material properties in the original system can be computed using the surrogate single-molecule simulation. In Section IV we benchmark our formalism against a well known result: the non-radiative relaxation of polariton and dark states. In Section V we present a pedagogical and intriguing application that reveals the power of our formalism, describing how to exploit polariton dynamics to obtain nonstatistical outcomes in photoproducts. Finally we summarize the work in Section VI.

II. THEORY

II.1. Hamiltonian and Multi-Configurational Wavefunction

Consider a system of N molecules collectively coupled to a single cavity mode. The Tavis-Cummings Hamiltonian, extended to include vibrational degrees of freedom missing from original models, can be written as (hereafter $\hbar = 1$)

$$\hat{H} = \sum_i^N \left(\hat{H}_m^{(i)} + \hat{H}_I^{(i)} \right) + \hat{H}_{cav}, \quad (1)$$

where

$$\begin{aligned} \hat{H}_m^{(i)} &= -\frac{1}{2\mu} \frac{\partial^2}{\partial q_i^2} + V_g(q_i)|g_i\rangle\langle g_i| + V_e(q_i)|e_i\rangle\langle e_i|, \\ \hat{H}_{cav} &= \omega_c \hat{a}^\dagger \hat{a}, \quad \hat{H}_I^{(i)} = g(|e_i\rangle\langle g_i|\hat{a} + |g_i\rangle\langle e_i|\hat{a}^\dagger), \end{aligned}$$

are the Hamiltonians for the i th molecule, the cavity mode, and the interaction between them. Here, $|g_i\rangle$ and $|e_i\rangle$ are the molecular ground and excited electronic states, $V_{g/e}(q_i)$ are the ground and excited Potential Energy Surfaces (PES), \hat{a} is the photon annihilation operator, and q_i is the vector of all molecular vibrations of molecule i . When the PESs are harmonic, the model above reduces to the Holstein-Tavis Cummings model, which has been subject of recent studies [20, 31]. For the time being, we assume there is no disorder, neglect intermolecular interactions, and use the rotating wave approximation by considering the single molecule coupling strength g to be much smaller than the bare photon frequency ω_c . Finally, we also ignore (non-radiative) couplings between the molecular ground and excited states

whose PESs can form conical intersections [33, 34]. Under these hypotheses, the excitation number [sum of electronic excitations (Frenkel excitons) and photon number] is conserved. In particular, in this article we shall focus on the so-called first-excitation manifold, which affords a position-representation ansatz of the form,

$$|\Psi(t)\rangle = \psi^{(0)}(\vec{q}, t)|1\rangle + \sum_i^N \psi^{(i)}(\vec{q}, t)|e_i\rangle, \quad (2)$$

with the electron-photon states $|e_i\rangle = |g_1, g_2, \dots, e_i, \dots, g_N, 0_{ph}\rangle$ and $|1\rangle = |g_1, g_2, \dots, g_N, 1_{ph}\rangle$, and the vibrational wavefunctions

$$\psi^{(0)}(\vec{q}, t) = \sum_{j_1}^m \sum_{j_2}^m \cdots \sum_{j_N}^m A_{j_1 j_2 \dots j_N}^{(0)}(t) \prod_{k=1}^N \varphi_{j_k}(q_k), \quad (3)$$

and

$$\psi^{(i)}(\vec{q}, t) = \sum_{j_1}^m \sum_{j_2}^m \cdots \sum_{j_N}^m A_{j_1 j_2 \dots j_N}^{(i)}(t) \phi_{j_i}(q_i) \prod_{k \neq i}^N \varphi_{j_k}(q_k). \quad (4)$$

In this expansion, multiconfigurational vibrational wavefunctions ψ are built with sets of m single particle orthonormal functions $\varphi_{j_i}(q_i)$ and $\phi_{j_i}(q_i)$, respectively, that are equal for identical molecules. In this work, we choose such functions to be the eigenstates of the molecular Hamiltonian $\hat{H}_m^{(i)}$. The total wavefunction becomes exact as $m \rightarrow \infty$.

II.2. Exploiting Permutational Symmetries

Since the Hamiltonian is invariant under the permutation of any pair of molecules α and κ , having an initial state such that $P_{\alpha\kappa}|\Psi(0)\rangle = |\Psi(0)\rangle$, implies permutation relations between the coefficients of the wavefunction. For the photonic and excitonic wavefunctions $\psi^{(0)}$ and $\psi^{(i)}$ we have,

$$\begin{aligned} A_{j_1 j_2 \dots j_\kappa \dots j_\nu \dots j_N}^{(0)}(t) &= A_{j_1 j_2 \dots j_\nu \dots j_\kappa \dots j_N}^{(0)}(t), \\ A_{j_1 j_2 \dots j_\kappa \dots j_i \dots j_\nu \dots j_N}^{(i)}(t) &= A_{j_1 j_2 \dots j_\nu \dots j_i \dots j_\kappa \dots j_N}^{(i)}(t). \end{aligned} \quad (5)$$

Additionally, there are permutations between coefficients of different excitons, given the interaction of the molecules with the cavity is assumed identical,

$$A_{j_1 j_2 \dots j_i \dots j_{i'} \dots j_N}^{(i)}(t) = A_{j_1 j_2 \dots j_{i'} \dots j_i \dots j_N}^{(i')}(t). \quad (6)$$

This means that every coefficient of the electronic state i' can be obtained directly from those in the electronic state i . In other words, Eqs. 5 and 6 yield the crucial observation that it is enough to calculate the dynamics

of a single excitonic state to know the evolution of all of them. Moreover, the vibrational states of the ensemble of molecules can be completely characterized by specifying the number of molecules in each vibrational state; therefore the number of vibrational degrees of freedom also reduces drastically. The ground and excited state coefficients can be written in terms of permutationally-symmetric states,

$$\begin{aligned} A_{j_1 j_2 j_3 \dots j_N}^{(0)} &\rightarrow A_{N_1 N_2 \dots N_m}^{(0)} \\ A_{j_1 j_2 j_3 \dots j_N}^{(i)} &\rightarrow A_{j_1 N_1 N_2 \dots N_m}^{(1)}, \end{aligned} \quad (7)$$

where N_k is the number of ground state molecules in the vibrational state k . This new notation removes the information about the state of each specific molecule ($A_{j_1 N_1 N_2 \dots N_m}^{(1)}$ represents a state where one molecule is in the electronic excited state in the vibrational state j_1 , while the other $N - 1$ molecules are distributed among all the vibrational states via $\{N_k\}$, $\sum_k N_k = N - 1$). For the photonic coefficients $A_{N_1 N_2 \dots N_m}^{(0)}$, the restriction is $\sum_k N_k = N$. For the vibrational wavefunction $\psi^{(0)}$ not all m^N configurations are unique but only $\binom{N+m-1}{N}$, (see Appendix for an illustrative example). Using similar analysis we conclude a reduction of the total wavefunction in Eq. 2 from $(N+1)m^N$ to $\binom{N+m-1}{N} + m\binom{N+m-2}{N-1}$ configurations. We will make use of these simplifications to redefine the equations of motion. Such analysis is general and can also be done for higher excitation manifolds. In broad terms, the number of coefficients increases with the number of excitations due to permutations between electronically excited molecules; however after the number of excitations is half of the number of molecules this trend reverses.

The EoM for the coefficients can be obtained by using the Dirac-Frenkel variational principle, or simply by inserting the ansatz wavefunction into the Time-Dependent Schrödinger Equation. Rewriting the ansatz as $|\Psi(t)\rangle = \sum_J^{m^N} A_J^{(0)}(t) \Phi_J^{(0)}|1\rangle + \sum_i \sum_J^{m^N} A_J^{(i)}(t) \Phi_J^{(i)}|e_i\rangle$ the EoM become (hereafter, $\hbar = 1$) [35]

$$i\dot{A}_J^{(i)}(t) = \sum_{i'} \sum_L \langle \Phi_J^{(i)} | \hat{H} | \Phi_L^{(i')} \rangle A_L^{(i')}(t). \quad (8)$$

Since Eq. 1 ignores couplings between the molecules in the absence of the photon mode, $\langle \Phi_J^{(i)} | \hat{H}_I | \Phi_L^{(i')} \rangle = 0$ for $i, i' \neq 0$. Furthermore,

$$\langle \Phi_J^{(i)} | \hat{H}_I | \Phi_L^{(0)} \rangle = g \langle \phi_{j_i} | \varphi_{l_i} \rangle \prod_{k \neq i}^N \delta_{j_k l_k}. \quad (9)$$

With these considerations, Eq. 8 becomes,

$$\begin{aligned} i\dot{A}_{j_1 j_2 \dots j_i \dots j_N}^{(i)}(t) &= \left(\sum_{i' \neq i}^N E_{g, j_{i'}} + E_{e, j_i} \right) A_{j_1 j_2 \dots j_i \dots j_N}^{(i)}(t) \\ &\quad + g \sum_{l_i} \langle \phi_{j_i} | \varphi_{l_i} \rangle A_{j_1 j_2 \dots l_i \dots j_N}^{(0)}(t) \\ i\dot{A}_{j_1 j_2 \dots j_N}^{(0)}(t) &= \left(\sum_{i'}^N E_{g, j_{i'}} + \omega_c \right) A_{j_1 j_2 \dots j_N}^{(0)}(t) \\ &\quad + g \sum_{i=1}^N \sum_{l_i} \langle \varphi_{j_i} | \phi_{l_i} \rangle A_{j_1 j_2 \dots l_i \dots j_N}^{(i)}(t). \end{aligned} \quad (10)$$

The last equation can be simplified using Eqs. 7 to write the dynamics in terms of permutationally-symmetric states:

$$\begin{aligned} i\dot{A}_{l N_1 N_2 \dots N_m}^{(1)}(t) &= \left(\sum_{k=1}^m N_k E_{g, k} + E_{e, l} \right) A_{l N_1 N_2 \dots N_m}^{(1)}(t) \\ &\quad + g \sum_k \langle \phi_l | \varphi_k \rangle A_{N_1 N_2 \dots N_k + 1 \dots N_m}^{(0)}(t) \\ i\dot{A}_{N_1 N_2 \dots N_m}^{(0)}(t) &= \left(\sum_{k=1}^m N_k E_{g, k} + \omega_c \right) A_{N_1 N_2 \dots N_m}^{(0)}(t) \\ &\quad + \sum_{k=1}^m N_k g \sum_{l=1}^m \langle \varphi_k | \phi_l \rangle A_{l N_1 \dots N_k - 1 \dots N_m}^{(1)}(t). \end{aligned} \quad (11)$$

The first equation represents the absorption of the photon that takes a molecule from the state $\varphi_k|g\rangle$ into the state $\phi_l|e\rangle$. The second equation describes the conjugate process. To summarize, the EoM in Eq. 11 are the main formal results of this article, which arise upon applying the permutational symmetries in Eqs. 5 and 6.

II.3. Structure of the Wavefunction

Even though Eqs. 11 are exact and represent a significant improvement over Eqs. 10, they also allows us to systematically introduce approximations by virtue of the factors N_k , which represent the number of ground state molecules in the vibrational state k . For initial states in which one of the values N_k is exceptionally large, the dynamics is such that N_k is almost conserved, as discussed below. As an example, assume we start with all the molecules in their ground vibrational state and 1 photon in the cavity mode, i.e., $A_{N 0 \dots 0}^{(0)}(0) = 1$. Thus, we can simplify even more our notation by only reporting the number of such vibrational excitations. By renormalizing the amplitudes we can recover the basis used by Spano [23]:

$$\begin{aligned}
\tilde{A}_0^{(0)}(t) &= A_{N00\dots 0}^{(0)}(t), \\
\tilde{A}_{l0}^{(1)}(t) &= \sqrt{N} A_{l(N-1)0\dots 0}^{(1)}(t), \\
\tilde{A}_k^{(0)}(t) &= \sqrt{N} A_{(N-1)\dots 1_k\dots 0}^{(0)}(t), \\
\tilde{A}_{lk}^{(1)}(t) &= \sqrt{N(N-1)} A_{l(N-2)\dots 1_k\dots 0}^{(1)}(t), \\
\tilde{A}_{k\neq k'}^{(0)}(t) &= \sqrt{N(N-1)} A_{(N-2)\dots 1_k\dots 1_{k'}\dots 0}^{(0)}(t), \\
\tilde{A}_{kk}^{(0)}(t) &= \sqrt{\frac{N(N-1)}{2}} A_{(N-2)\dots 2_k\dots 0}^{(0)}(t), \tag{12}
\end{aligned}$$

$$\begin{aligned}
i\dot{\tilde{A}}_0^{(0)}(t) &= \omega_c \tilde{A}_0^{(0)}(t) + g\sqrt{N} \sum_{l=1}^m \langle \varphi_1 | \phi_l \rangle \tilde{A}_{l0}^{(1)}(t) \\
i\dot{\tilde{A}}_{l0}^{(1)}(t) &= \omega_{eg,l} \tilde{A}_{l0}^{(1)}(t) + g\sqrt{N} \langle \phi_l | \varphi_1 \rangle \tilde{A}_0^{(0)}(t) + g \sum_{k=2}^m \langle \phi_l | \varphi_k \rangle \tilde{A}_k^{(0)}(t) \\
i\dot{\tilde{A}}_k^{(0)}(t) &= (\omega_{g,k} + \omega_c) \tilde{A}_k^{(0)}(t) + g\sqrt{N-1} \sum_{l=1}^m \langle \varphi_1 | \phi_l \rangle \tilde{A}_{lk}^{(1)}(t) + g \sum_{l=1}^m \langle \varphi_k | \phi_l \rangle \tilde{A}_{l0}^{(1)}(t) \\
i\dot{\tilde{A}}_{lk}^{(1)}(t) &= (\omega_{eg,l} + \omega_{g,k}) \tilde{A}_{lk}^{(1)}(t) + g\sqrt{N-1} \langle \phi_l | \varphi_1 \rangle \tilde{A}_k^{(0)}(t) + g \sum_{k' \neq k} \langle \phi_l | \varphi_{k'} \rangle \tilde{A}_{kk'}^{(0)}(t) + \sqrt{2}g \langle \phi_l | \varphi_k \rangle \tilde{A}_{kk}^{(0)}(t) \\
&\vdots \tag{13}
\end{aligned}$$

where we have removed a constant $NE_{g,1}$ and defined $\omega_{eg,l} = E_{e,l} - E_{g,1}$ and $\omega_{g,k} = E_{g,k} - E_{g,1}$. The first equation reveals that the initial photonic state $\tilde{A}_0^{(0)}(t)$ is strongly coupled to states in which one molecule is electronically excited while the rest remain in their ground electronic and vibrational states $\tilde{A}_{l0}^{(1)}(t)$. However, the second equation reveals that such excited state can either emit back into the initial state (with no phonons), or can create states in which there is a vibrational excitation in one of the ground state molecules $\tilde{A}_k^{(0)}(t)$ upon emission. The first of these two processes depends on the collective light-matter coupling $\sqrt{N}g$, while the second one depends on the single-molecule light-matter coupling g . This structure is repeated throughout the system of equations: coupling between states conserving the number of molecules with phonons is collective, while processes that increase the number of such molecules are proportional to the single-molecule coupling. It is interesting to note that this phenomenon is well-known in the literature of molecular aggregates. In particular, for J-aggregates, Spano and Yamagata [36] have noted that the ratio of the photoluminescence into the electronic ground state with no phonons versus that into the electronic ground state with one phonon is proportional to the coherence length N of the aggregate. While this phenomenon is thus routinely used as a spectroscopic probe for N , in our case, it is used to drastically simplify the simulations

and so on. With this final notation, the EoM in Eq. 11 become,

of molecular polaritons, as explained below.

Assuming we have a large number of molecules we can treat the mixing of states with differing number of ground state molecules with phonons perturbatively, with the *single*-molecule light-matter coupling g as the perturbation. This is schematically represented in the next figure.

In the limit where $g \rightarrow 0$ or $N \rightarrow \infty$ (while keeping $\sqrt{N}g$ constant), which is the regime that interests us, the number of ground state molecules that support vibrational excitations is conserved during the dynamics. For our initial state, the zeroth-order approximation implies that the wavefunction is described only by the basis states of the first block of Fig. 1. The first-order approximation allows states to the right of the first block to contribute to the wavefunction, states where one ground state molecule has phonons. The timescale at which the first-order terms contribute is generally much longer than the ultrafast vibrational dynamics on each excited molecule. The exact wavefunction is recovered as one spans the entire Hilbert space from left to right in Fig. 1, but as can be appreciated, there are only a few molecules with phonons in the electronic ground state for large N , even for long times of interest, justifying the convenience of the shorthand notation in Eq. 12.

Although the fact that there is no disorder in the system is central for the permutational symmetries of Eqs. 5 and 6 to hold, addition of different types of molecules can be done without dramatically increasing the compu-

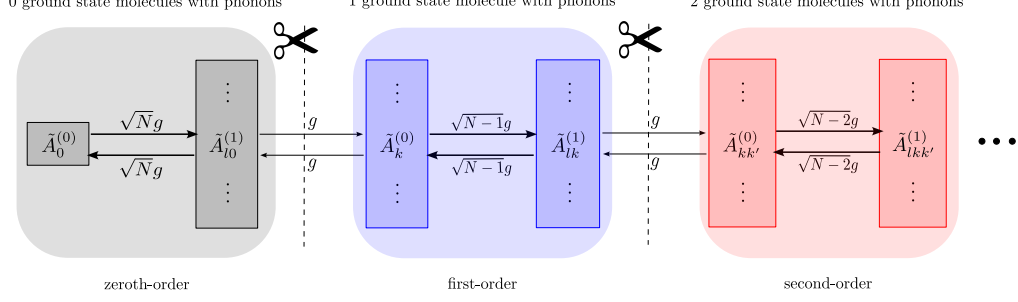


FIG. 1. Structure of the equations of motion and time-dependent wavefunction of molecular-polaritonic system in the collective strong coupling regime. Zeroth-order approximation in g corresponds to restricting the dynamics to the states with 0 ground state molecules with vibrational excitations, while the first-order approximation allows the dynamics to create phonons in 1 molecule. Restriction to the zeroth (first)-order approximation drastically simplifies the simulation to only one (two) effective molecule(s) coupled to a cavity.

tational cost since permutational symmetries still apply for each type. The renormalization of the coefficients associated to each species as in Eq. 12 will depend on their concentration. Similarly, disorder due to inhomogeneous broadening or spacial variation of the coupling to the photon mode can be included by adding new types of molecules for each value that is sampled according to the corresponding distribution of excitonic frequencies or interaction strength. Notice that the computational cost is still reduced significantly in this case since the distribution can be discretized into a small number of bins.

II.4. Zeroth-Order Approximation

Let us assume that temperature $T = 0$, meaning our initial state in the original notation is given by

$A_{111\dots 1}^{(0)}(0) = 1$. The time-dependent wavefunction (see Eq. 2) at the zeroth-order approximation is given by the following vibrational wavefunctions

$$\begin{aligned}\psi^{(0)}(\vec{q}, t) &= A_{11\dots 1}^{(0)}(t) \prod_k \varphi_1(q_k) \quad \text{and} \\ \psi^{(i)}(\vec{q}, t) &= \sum_{j_i} A_{j_i 1\dots 1}^{(1)}(t) \phi_{j_i}(q_i) \prod_{k \neq i} \varphi_1(q_k).\end{aligned}\quad (14)$$

By using the renormalized permutationally-symmetric coefficients, the EoM in Eq. 13 transform into those of an *effective* single molecule strongly coupled to the cavity mode (with effective coupling $\sqrt{N}g$),

$$i \begin{pmatrix} \dot{\tilde{A}}_0^{(0)}(t) \\ \dot{\tilde{A}}_{10}^{(1)}(t) \\ \dot{\tilde{A}}_{20}^{(1)}(t) \\ \vdots \\ \dot{\tilde{A}}_{m0}^{(1)}(t) \end{pmatrix} = \begin{pmatrix} \omega_c & g\sqrt{N}\langle\varphi_1|\phi_1\rangle & g\sqrt{N}\langle\varphi_1|\phi_2\rangle & \cdots & g\sqrt{N}\langle\varphi_1|\phi_m\rangle \\ g\sqrt{N}\langle\phi_1|\varphi_1\rangle & \omega_{eg,1} & 0 & \cdots & 0 \\ g\sqrt{N}\langle\phi_2|\varphi_1\rangle & 0 & \omega_{eg,2} & \cdots & 0 \\ \vdots & \vdots & \vdots & \cdots & \vdots \\ g\sqrt{N}\langle\phi_m|\varphi_1\rangle & 0 & 0 & \cdots & \omega_{eg,m} \end{pmatrix} \begin{pmatrix} \tilde{A}_0^{(0)}(t) \\ \tilde{A}_{10}^{(1)}(t) \\ \tilde{A}_{20}^{(1)}(t) \\ \vdots \\ \tilde{A}_{m0}^{(1)}(t) \end{pmatrix}. \quad (15)$$

Eq. 15 is consistent with previous results where an impurity (in this case the optical mode) coupled to a large environment can be simplified into an impurity interacting with an effective harmonic bath that includes the relevant frequencies of the environment [37]; in this case the optical transitions of an individual molecule. Alternatively, it is also consistent with the classical optics treatment of polaritons arising as the result of a photonic oscillator

coupling to a set of effective oscillators representing the molecular transitions [38, 39]. The effective zeroth-order Hamiltonian in Eq. 15 can be compactly written as,

$$\begin{aligned}\hat{H}^{(0)} &= \left(\mathbb{P} \hat{H}_g \mathbb{P} + \omega_c \right) |1\rangle\langle 1| + \hat{H}_e |e\rangle\langle e| \\ &+ g\sqrt{N} (|e\rangle\langle 1| + |1\rangle\langle e|),\end{aligned}\quad (16)$$

with $\hat{H}_{g/e} = \frac{1}{2\mu}\hat{p}^2 + V_{g/e}(\hat{q})$, and the projector over the ground vibrational state $\mathbb{P} = |\varphi_1\rangle\langle\varphi_1|$. Alternatively, we can rewrite Eq. 15 in a form that is better suited for implementation in quantum dynamics methods such as MCTDH [35, 40],

$$i \begin{pmatrix} \dot{\psi}_{ph}(q, t) \\ \dot{\psi}_{exc}(q, t) \end{pmatrix} = \begin{pmatrix} \mathbb{P}\hat{H}_g\mathbb{P} + \omega_c & g\sqrt{N} \\ g\sqrt{N} & \hat{H}_e \end{pmatrix} \begin{pmatrix} \psi_{ph}(q, t) \\ \psi_{exc}(q, t) \end{pmatrix}, \quad (17)$$

with the photonic and excitonic wavefunctions

$$\psi_{ph}(q, t) = \tilde{A}_0^{(0)}(t)\varphi_1(q), \quad \psi_{exc}(q, t) = \sum_j^m \tilde{A}_{j0}^{(1)}(t)\phi_j(q). \quad (18)$$

These wavefunctions can be used to recover the original time-dependent many-body wavefunctions in Eq. 14.

At this stage, there are two important details to keep in mind. First, the artificial effective molecule in the ground state is only allowed to be in its ground vibrational state (no phonons). The physical intuition for this is simple: imagine the molecules have been collectively excited at their Franck-Condon (FC) configurations by the cavity field; each of them can in principle re-emit such energy into the cavity creating any vibrational state of

their ground electronic state. However, only when they go back to their vibrational ground state the number of ground state molecules with phonons is conserved and the process becomes superradiant.

This seemingly unremarkable observation has an important implication: it states that single-molecule polariton simulations are not applicable to the collective regime unless the light-matter coupling is restricted to the FC region (where the vibrational ground state $\varphi_1(q)$ has significant amplitude). However, as Eq. 17 reveals, such simulations can be simply adjusted for the collective regime by the appropriate inclusion of the projector \mathbb{P} ; see Fig. 2. This projector can be readily implemented in various ways (e.g., by restricting the vibrational basis in the ground state to $|\varphi_1\rangle$, by projecting the light-matter coupling, among several options). Second, the results of this section are exact in the thermodynamic ($N \rightarrow \infty$) limit because they imply $g \rightarrow 0$. We next analyze the first-order approximation, where the wavefunction now has states with amplitude of the order of g .

II.5. First-Order Approximation and Beyond

Proceeding analogously, the EoM *up to* first order can be written as

$$i \begin{pmatrix} \dot{\tilde{A}}_0^{(0)}(t) \\ \dot{\tilde{A}}_{10}^{(1)}(t) \\ \dot{\tilde{A}}_1^{(0)}(t) \\ \dot{\tilde{A}}_{11}^{(1)}(t) \end{pmatrix} = \begin{pmatrix} \omega_c & g\sqrt{N}\langle\varphi_1|\phi_1\rangle & 0 & 0 \\ g\sqrt{N}\langle\phi_1|\varphi_1\rangle & \omega_{eg,1} & \boxed{g\langle\phi_1|\varphi_2\rangle} & 0 \\ 0 & \boxed{g\langle\varphi_2|\phi_1\rangle} & \omega_{g,2} + \omega_c & g\sqrt{N-1}\langle\varphi_1|\phi_1\rangle \\ 0 & 0 & g\sqrt{N-1}\langle\phi_1|\varphi_1\rangle & \omega_{g,2} + \omega_{eg,1} \end{pmatrix} \begin{pmatrix} \tilde{A}_0^{(0)}(t) \\ \tilde{A}_{10}^{(1)}(t) \\ \tilde{A}_1^{(0)}(t) \\ \tilde{A}_{11}^{(1)}(t) \end{pmatrix},$$

where we consider the case $m = 1$ for illustration purposes. As in the previous section, the effective Hamiltonian can be written in a more compact form using projection operators,

$$\begin{aligned} \hat{H}^{(1)} = & \left(\mathbb{P}_1 \hat{H}_{g,1} \mathbb{P}_1 + \mathbb{P}_2 \hat{H}_{g,2} \mathbb{P}_2 + \omega_c \right) |1, 0\rangle\langle 1, 0| + \left(\hat{H}_{e,1} + \mathbb{P}_2 \hat{H}_{g,2} \mathbb{P}_2 \right) |e, 0\rangle\langle e, 0| \\ & + \left(\mathbb{Q}_1 \hat{H}_{g,1} \mathbb{Q}_1 + \mathbb{P}_2 \hat{H}_{g,2} \mathbb{P}_2 + \omega_c \right) |1, 1\rangle\langle 1, 1| + \left(\mathbb{Q}_1 \hat{H}_{g,1} \mathbb{Q}_1 + \hat{H}_{e,2} \right) |e, 1\rangle\langle e, 1| \\ & + g\sqrt{N} (|e, 0\rangle\langle 1, 0| + |1, 0\rangle\langle e, 0|) + g\sqrt{N-1} (|e, 1\rangle\langle 1, 1| + |1, 1\rangle\langle e, 1|) + g (|e, 0\rangle\langle 1, 1| + |1, 1\rangle\langle e, 0|), \end{aligned} \quad (19)$$

where $\mathbb{Q}_i = \mathbb{1}_{vib,i} - \mathbb{P}_i$. When compared to $\hat{H}^{(0)}$ in Eq. 16 we notice the emergence of a second label for the effective electronic state corresponding to the number of ground state molecules with phonons. We make use of this Hamiltonian in Section IV.

Although higher order approximations would require the addition of more electronic-photonic states, going beyond the first-order approximation will provide infor-

mation about phenomena with rates that scale as $1/N^k$ with $k > 1$ (see Section IV). Although some of those phenomena might become relevant when a small number of molecules is considered, we will defer their exploration for future works.

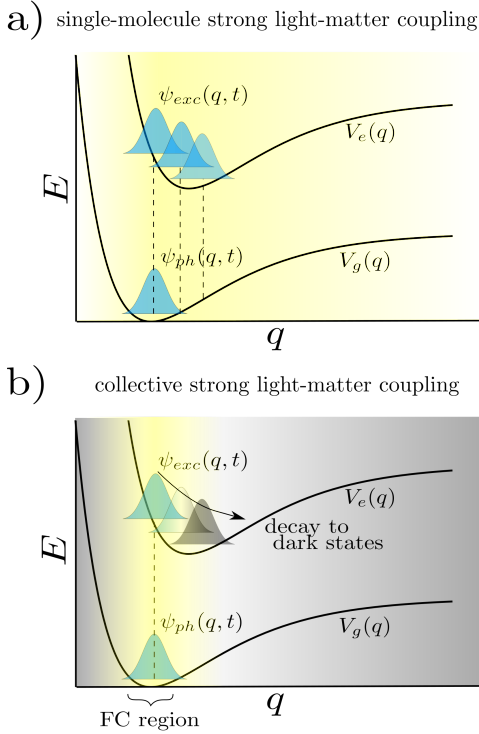


FIG. 2. (a) For a cavity containing a single-molecule, light-matter coupling (denoted in yellow) has the ability to modify nuclear dynamics throughout all configurations q . (b) This situation contrasts with a cavity containing many molecules, where collective light-matter coupling is localized at the FC region. Nuclear displacement away from this region is equivalent to decay of polaritons into dark states, as explained in Section III.2.1.

III. OBSERVABLES IN THE ZERO-ORDER APPROXIMATION

Observables of the real system must be calculated using $|\Psi(t)\rangle$ and not directly using $|\tilde{\Psi}(t)\rangle$. However, there are particular observables for which both wavefunctions provide the same answer. This will depend on whether the observable is local or collective. For pedagogical purposes, throughout this section, we assume the zeroth-order approximation.

III.1. Local Properties

Hereafter, we define local properties to be quantities that only depend on one single molecule (e.g. a chemical reaction) or the photon field alone.

III.1.1. Chemical Properties:

Consider a local observable $\hat{\Omega}^{(i)}$ that depends only on degrees of freedom of molecule i . As an example, assume we are interested in the nuclear dynamics in the excited

state $\hat{\Omega}^{(i)} = \hat{q}_i |e_i\rangle \langle e_i|$. Using the zeroth-order wavefunction in Eq. 14 we obtain

$$\langle \Psi(t) | \hat{q}_i | e_i \rangle \langle e_i | \Psi(t) \rangle = \frac{1}{N} \langle \tilde{\Psi}(t) | \hat{q} | e \rangle \langle e | \tilde{\Psi}(t) \rangle. \quad (20)$$

This is a remarkable result because it demonstrates that the excited-state dynamics of N molecules collectively coupled to a cavity mode (described by $|\Psi(t)\rangle$) is identical to the dynamics of an effective single molecule strongly coupled to a cavity (described by $|\tilde{\Psi}(t)\rangle$), except for a constant $1/N$ dilution factor. This factor is just a consequence of using a single photon to alter the excited state dynamics of N molecules. The probability of *any* molecule being at the configuration q is the same as that of the single effective molecule strongly coupled to the cavity. However, we emphasize that the effective molecule is not allowed to have phonons while it is in the ground state, a restriction which can introduce significant differences compared to standard single-molecule calculations.

An important corollary of the above analysis is that effects predicted using single-molecule models might actually occur in the collective regime if they rely on changes in the excited PES at the FC region, but not the ones relying on changes beyond. This conclusion is consistent with a recent work by Cui and Nitzan [41], who concluded that excited state dynamics in polaritonic systems is highly dominated by states that are reachable from the ground electronic state. Yet, we propose that modifications of chemical dynamics that occur on a timescale longer than the decay of the initially prepared excitations can occur in an N -independent manner if they dramatically depend on the ultrafast polariton-modified dynamics at the FC region. In section V we present such an example.

III.1.2. Optical properties:

Another set of properties that are equivalent in the single molecule and $N \rightarrow \infty$ case are those that can be extracted only from the dynamics of the field. For example, the linear transmission, absorption and reflection spectra can be calculated from the photon autocorrelation function $c(t)$. In the zeroth-order approximation, it can be shown that $c(t) = \langle \Psi(0) | \Psi(t) \rangle = \langle \tilde{\Psi}(0) | \tilde{\Psi}(t) \rangle$, where $|\tilde{\Psi}(0)\rangle = \varphi_0(q)|1\rangle$ is the photonic state. This is consistent with previous work by the Keeling group [31, 32].

III.2. Non-Local Properties

Another set of observables consists of operators that are delocalized across several molecules or depend on both molecular and optical degrees of freedom. Some of the most common observables of this kind are the populations of the polariton and dark-states. Such observables can be obtained with the effective single-molecule model

but not from its reduced electronic-photonic density matrix, as we will show next.

III.2.1. Polariton and Dark-States Populations

Let us write the expectation value of an arbitrary electronic-photonic operator $\langle \hat{\Omega} \rangle = \text{Tr} [\hat{\rho} \hat{\Omega}]$ in terms of the reduced density matrix of the effective single molecule system $\hat{\rho}$:

$$\begin{aligned} \langle \hat{\Omega} \rangle = \text{Tr} [\hat{\rho} \hat{\Omega}] &= \sum_{ij} \rho_{ij} \Omega_{ji} = \tilde{\rho}_{11} \Omega_{11} + \tilde{\rho}_{1e} \sum_{i=1}^N \frac{1}{\sqrt{N}} \Omega_{1e_i} \\ &+ \tilde{\rho}_{e1} \sum_{i=1}^N \frac{1}{\sqrt{N}} \Omega_{e_i 1} + \tilde{\rho}_{ee} \frac{1}{N} \sum_{i=1}^N \Omega_{e_i e_i} \\ &+ \frac{1}{N} \langle \tilde{\Psi}(t) | \tilde{\Psi}_{FC} \rangle \langle \tilde{\Psi}_{FC} | \tilde{\Psi}(t) \rangle \left(\sum_{i,i' \neq i} \Omega_{e_i e_{i'}} \right), \quad (21) \end{aligned}$$

where we have identified $|\tilde{\Psi}_{FC}\rangle = \varphi_1(q)|e\rangle$ as the FC wavepacket. The above equation implies that the reduced density matrix $\tilde{\rho}$ of the effective single molecule is, in general, not enough to calculate any delocalized molecular observables since the last term of Eq. 23 refers to the projection of the wavefunction onto the FC wavepacket, which corresponds to the inter-exciton coherences:

$$\langle e_i | \hat{\rho}(t) | e_{i'} \rangle = \frac{1}{N} \langle \tilde{\Psi}(t) | \tilde{\Psi}_{FC} \rangle \langle \tilde{\Psi}_{FC} | \tilde{\Psi}(t) \rangle. \quad (22)$$

An example, let $\hat{\Omega} = |P\rangle\langle P|$, with $|P\rangle = c_0|1\rangle + c_1|B\rangle$ (where $|B\rangle = \frac{1}{\sqrt{N}} \sum_{i=1}^N |e_i\rangle$ is the totally-symmetric excitonic state) being one of the polariton states. Using Eq. 21, population of this state is calculated to be

$$\begin{aligned} \langle \Psi(t) | P \rangle \langle P | \Psi(t) \rangle &\approx |c_0|^2 \tilde{\rho}_{11}(t) + c_0^* c_1 \tilde{\rho}_{1e} + c_1^* c_0 \tilde{\rho}_{e1} \\ &+ |c_1|^2 \langle \tilde{\Psi}(t) | \tilde{\Psi}_{FC} \rangle \langle \tilde{\Psi}_{FC} | \tilde{\Psi}(t) \rangle. \quad (23) \end{aligned}$$

Similarly, dark states can be written as $|D\rangle = \sum_i c_i |e_i\rangle$, with $|c_1| = |c_2| = \dots = |c_N| = 1/\sqrt{N}$, $\sum_{i=1}^N c_i = 0$, and $\Omega_{e_i e_j} = \langle e_i | D \rangle \langle D | e_j \rangle = c_i c_j^*$ (i.e., they are chosen orthogonal to the $|P\rangle$ states, so here we take them to be the Fourier combinations of excitons that are orthogonal to $|B\rangle$; see for instance [42]). This leads to

$$\langle \Psi(t) | D \rangle \langle D | \Psi(t) \rangle = \frac{1}{N} \langle \tilde{\Psi}(t) | e \rangle (1 - |\varphi_1\rangle\langle\varphi_1|) \langle e | \tilde{\Psi}(t) \rangle. \quad (24)$$

Notice that this calculation is identical for every dark state in the chosen basis, therefore the population in the dark-state manifold yields

$$\begin{aligned} \sum_k^{N-1} \langle |D\rangle \langle D| \rangle &\approx 1 - \langle \tilde{\Psi}(t) | 1 \rangle \langle 1 | \tilde{\Psi}(t) \rangle \\ &- \langle \tilde{\Psi}(t) | \tilde{\Psi}_{FC} \rangle \langle \tilde{\Psi}_{FC} | \tilde{\Psi}(t) \rangle, \quad (25) \end{aligned}$$

where we have made $\frac{N-1}{N} \approx 1$ since the zeroth-order approximation becomes exact for $N \rightarrow \infty$. From this result, we can extract the intuitive interpretation that the bright state $|B\rangle$ in the N -molecule system corresponds to a FC wavepacket in the excited state of the effective single molecule, while the dark states correspond to the rest of the wavefunction whose nuclear configurations lie outside of the FC region.

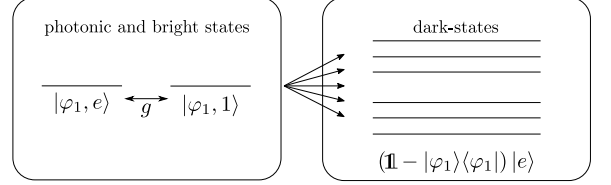


FIG. 3. Bright, photonic, and dark states in the effective zeroth-order approximation. Dark states in the single-molecule picture on the zeroth-order approximation correspond to vibrational states of the excited electronic state that are orthogonal to $|\varphi_1\rangle$.

For cases where the chemically relevant excited state dynamics involves fast changes of the nuclear configurations away from the FC point, excited state reactivity is essentially relaxation to dark-states. The question is whether the relaxation occurs along the reactive coordinate of interest (e.g., particular reactive dark-modes), or whether it occurs along orthogonal modes to it. Thus, we have derived a powerful design principle for polariton chemistry which has so far unjustifiably gathered little attention: the strategy is not to avoid decay into dark states, which seems inexorable in most cases, but to use strong coupling to control which dark states to target. In fact, using the zeroth-order approximation, we will illustrate some mechanisms to manipulate ratios for these relaxation pathways in Section V.

IV. POLARITON VIBRATIONAL RELAXATION

Previous work by del Pino and coworkers [43] addressed the relaxation dynamics of molecular polaritons using the Hamiltonian in Eq. 1 for a vibrational harmonic bath and linear vibronic coupling,

$$\begin{aligned} \hat{H}_m^{(i)} &= \sum_k \omega_{\nu,k} \hat{b}_k^{(i)\dagger} \hat{b}_k^{(i)} \\ &+ \left[\omega_{eg,1} + \sum_k \omega_{\nu,k} \sqrt{s_k} (\hat{b}_k^{(i)\dagger} + \hat{b}_k^{(i)}) \right] |e_i\rangle\langle e_i|. \quad (26) \end{aligned}$$

This model of relaxation is the single-photon mode simplification of a previous model by Litinskaya and Agranovich [44]. In the limit where vibronic coupling is much smaller than the collective light-matter coupling

and there is an energy-dense set of vibrational modes k , we can use our formalism to analytically derive relaxation rates by including a collection of local vibrational modes and using Fermi's Golden Rule with the vibronic couplings as the perturbation. Although such a result is already well known, it serves as a benchmark and illustration for our formalism. To unclutter the calculations, let us consider the case where the excitons and the cavity are in resonance ($\omega_c = \omega_{eg,1} = \omega$).

IV.1. Zeroth-Order Approximation: N -Independent Effects

Using Eq. 16, the model of relaxation in the zeroth-order approximation is given by the unperturbed and vibronic coupling Hamiltonians

$$\hat{H}^{(0)} = \hat{H}_0^{(0)} + \hat{H}_I^{(0)},$$

$$\begin{aligned} \hat{H}_0^{(0)} = & \omega|1,0\rangle\langle 1,0| + \left(\omega + \sum_k \omega_{\nu,k} \hat{b}_k^\dagger \hat{b}_k \right) |e\rangle\langle e| \\ & + \sqrt{N}g(|e,0\rangle\langle 1,0| + |1,0\rangle\langle e,0|), \end{aligned}$$

$$\hat{H}_I^{(0)} = \sum_k \omega_{\nu,k} \sqrt{s_k} \left(\hat{b}_k^\dagger + \hat{b}_k \right) |e\rangle\langle e|, \quad (27)$$

where we have used the Fock basis for the vibrational bath (which is the eigenbasis of the electronic ground-state vibrational Hamiltonian $\hat{H}_{g,i} = \sigma_k \omega_{\nu,k} (\hat{b}_{i,k} + \hat{b}_{i,k}^\dagger)$; the second index “0” means all vibrational modes k are empty; do not confuse this notation with that of Eq. 19). The eigenstates of $\hat{H}_0^{(0)}$ are trivial,

$$\begin{aligned} |\pm, 0\rangle &= \frac{1}{\sqrt{2}} (|e, 0\rangle \pm |1, 0\rangle) \\ |D, m\rangle &= |e, m > 0\rangle, \end{aligned} \quad (28)$$

where $m > 0$ denotes that at least one mode of the vibrational bath is not in the vacuum state. The eigenvalues are given by $\omega_{\pm,0} = \omega \pm g$ and $\omega_{D,m} = \omega + \sum_k \omega_{\nu,k} m_k$ respectively. Using Fermi's Golden Rule we can obtain

the following relaxation rates:

$$\begin{aligned} \Gamma_{D \leftarrow +} &= 2\pi \sum_m |\langle D, m | \hat{H}_1^{(0)} | +, 0 \rangle|^2 \delta(\omega_{D,m} - \omega_{+,0}) \\ &= \frac{2\pi}{2} \sum_k \omega_{\nu,k}^2 s_k \delta(g - \omega_{\nu,k}), \end{aligned} \quad (29)$$

$$\Gamma_{- \leftarrow +} = 2\pi |\langle -, 0 | \hat{H}^{(1)} | +, 0 \rangle|^2 \delta(2g) = 0, \quad (30)$$

$$\Gamma_{- \leftarrow D} = 2\pi |\langle -, 0 | \hat{H}^{(1)} | e, m \rangle|^2 \delta(2g - \sum_k \omega_{\nu,k} m_k) = 0, \quad (31)$$

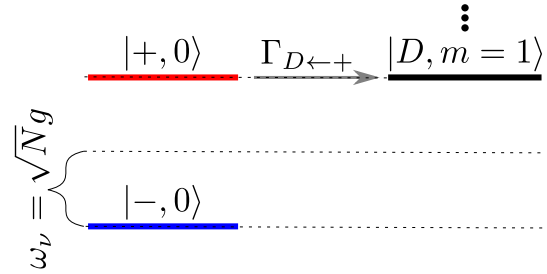


FIG. 4. Eigenstates of $\hat{H}_0^{(0)}$ and relaxation mechanism. Only states $|+, 0\rangle$ and $|d, m=1\rangle$ are resonantly coupled through vibronic coupling. $m=1$ means there is 1 phonon in one of the bath modes of the excited effective molecule.

where the last two rates are equal to 0 because the resonance condition is not fulfilled. A schematic representation of the relaxation dynamics is shown in Fig. 4.

Apart from missing a factor of $\frac{N-1}{N}$ in $\Gamma_{D \leftarrow +}$, the zeroth-order approximation correctly predicts the relaxation rate from upper polariton to dark states (which in this weak-vibronic coupling model in the effective single-molecule calculation, corresponds to the bare molecular exciton with a single phonon $|e, 1\rangle$), but disregards both the upper to lower polariton, and dark state to lower polariton rates [43]. This makes sense since the latter two are known to be proportional to $1/N$, and the zeroth-order approximation is exact for $N \rightarrow \infty$. Thus, for this simple model, the only relaxation process of relevance at ultrafast timescales is the downhill one *into* dark states.

IV.2. First-Order Approximation: $1/N$ Effects

By analogy with the previous section, we describe the vibrations with the eigenbases of the electronic ground-state vibrational Hamiltonians of the two molecules in the effective Hamiltonian up to the first-order approximation. Using Eq. 19, the relaxation model is described by the Hamiltonians

$$\begin{aligned}
\hat{H}^{(1)} &= \hat{H}_0^{(1)} + \hat{H}_1^{(1)}, \\
\hat{H}_0^{(1)} &= \omega |1, 0, 0, 0\rangle \langle 1, 0, 0, 0| + \sum_m \left(\omega + \sum_k \omega_{\nu,k} m_k \right) |e, 0, m, 0\rangle \langle e, 0, m, 0| + \sum_{m>0} \left(\omega + \sum_k \omega_{\nu,k} m_k \right) |1, 1, m, 0\rangle \langle 1, 1, m, 0| \\
&+ \sum_{m>0, n} \left(\omega + \sum_k \omega_{\nu,k} m_k + \sum_k \omega_{\nu,k} n_k \right) |e, 1, m, n\rangle \langle e, 1, m, n| + g\sqrt{N} (|1, 0, 0, 0\rangle \langle e, 0, 0, 0| + |e, 0, 0, 0\rangle \langle 1, 0, 0, 0|) \\
&+ g\sqrt{N-1} \sum_{m>0} (|1, 1, m, 0\rangle \langle e, 1, m, 0| + |e, 1, m, 0\rangle \langle 1, 1, m, 0|) + g \sum_{m>0} (|e, 0, m, 0\rangle \langle 1, 1, m, 0| + |1, 1, m, 0\rangle \langle e, 0, m, 0|), \\
\hat{H}_1^{(1)} &= \sum_k \omega_{\nu,k} \sqrt{s_k} (\hat{b}_{1,k}^\dagger + \hat{b}_{1,k}) |e, 0\rangle \langle e, 0| + \sum_k \omega_{\nu,k} \sqrt{s_k} (\hat{b}_{2,k}^\dagger + \hat{b}_{2,k}) |e, 1\rangle \langle e, 1|,
\end{aligned} \tag{32}$$

where the last two labels in the kets represent the vibrational states of molecules 1 and 2 in the aforementioned Fock basis, $\hat{b}_{i,k}$ is the annihilation operator for the vibrational excitations of molecule i , and $m > 0$ means $m_k > 0$ for at least one mode k . The eigenstates of $\hat{H}_0^{(1)}$ are given by

$$\begin{aligned}
|\pm, 0, 0\rangle &= \frac{1}{\sqrt{2}} (|1, 0, 0, 0\rangle \pm |e, 0, 0, 0\rangle) \\
|\pm, m > 0, 0\rangle &= \frac{1}{\sqrt{2}} |1, 1, m > 0, 0\rangle \\
&\pm \frac{1}{\sqrt{2}} \left(\sqrt{\frac{N-1}{N}} |e, 1, m > 0, 0\rangle + \frac{1}{\sqrt{N}} |e, 0, m > 0, 0\rangle \right) \\
|D, m > 0, 0\rangle &= \frac{1}{\sqrt{N}} |e, 1, m > 0, 0\rangle + \sqrt{\frac{N-1}{N}} |e, 0, m > 0, 0\rangle \\
|D, m > 0, n\rangle &= |e, 1, m > 0, n > 0\rangle,
\end{aligned}$$

with eigenvalues $\omega_{\pm,0,0} = \omega \pm g\sqrt{N}$, $\omega_{\pm,m,0} = \omega + \sum_k \omega_{\nu,k} n_k \pm g\sqrt{N}$, and $\omega_{D,m,n} = \omega + \sum_k \omega_{\nu,k} m_k + \sum_k \omega_{\nu,k} n_k$ respectively. We can use these states to calculate the rate from the upper polariton to the lower polariton using Fermi's Golden Rule to get

$$\begin{aligned}
\Gamma_{\leftarrow+} &= 2\pi \sum_m |\langle -, 0, 0 | \hat{H}_1^{(1)} | +, 0, 0 \rangle|^2 \delta(\omega_{-,0,0} - \omega_{+,0,0}) \\
&= \frac{2\pi}{4N} \sum_k \omega_{\nu,k}^2 s_k \delta(2\sqrt{N}g - \omega_{\nu,k}).
\end{aligned} \tag{33}$$

Similarly, we can recalculate the decay rate from the upper polariton into the dark states,

$$\begin{aligned}
\Gamma_{D\leftarrow+} &= 2\pi \sum_m |\langle D, m, 0 | \hat{H}_1^{(1)} | +, 0, 0 \rangle|^2 \delta(\omega_{+,0,0} - \omega_{D,m,0}) \\
&= \left(\frac{N-1}{N} \right) \pi \sum_k \omega_{\nu,k}^2 s_k \delta(\sqrt{N}g - \omega_{\nu,k}).
\end{aligned} \tag{34}$$

where we have recovered the $\frac{N-1}{N}$ factor missing from Eq. 29 in the zero-order approximation. The final state in the previous calculation can be used as initial state to describe the subsequent relaxation from the dark-states

into the lower polariton,

$$\begin{aligned}
\Gamma_{\leftarrow D} &= 2\pi \sum_{m'} |\langle -, m', 0 | \hat{H}_1^{(1)} | -, 0, 0 \rangle|^2 \delta(\omega_{-,0,0} - \omega_{D,m=1,0}) \\
&= \left(\frac{N-1}{N^2} \right) \pi \sum_k \omega_{\nu,k}^2 s_k \delta(\sqrt{N}g - \omega_{\nu,k}),
\end{aligned} \tag{35}$$

where the factor $\frac{N-1}{N^2}$ can be approximated as $1/N$. We suspect this factor will become exactly $1/N$ if higher order approximations are considered. The schematic representation of these processes is shown in Figs. 5 and 6.

We conclude once more that in order to get dynamical effects that do not vanish in the thermodynamic limit it is sufficient to use the zeroth-order approximation. Likewise, to obtain slow rates proportional to $1/N$ (e.g. $\Gamma_{\leftarrow+}$, $\Gamma_{\leftarrow D}$) we only need to go to the first-order approximation. It is unlikely that we would need to go to higher-order approximations for microcavity polaritons, or even for polaritons arising in plasmonic antennas, where $N = 100 - 1000$ [45], although if strong coupling can be demonstrated with smaller N values, those corrections could start mattering.

IV.3. Finite Temperature effects

In the previous sections we have only dealt with transitions from higher to lower lying polaritonic or dark states. To calculate rates such as $\Gamma_{D\leftarrow-}$ we need to consider all possible initial states allowed by thermal fluctuations. In general, such states involve breaking of the symmetry that is essential for the reduction of the dimensionality in Eqs. 11. Therefore, at the current stage this formalism cannot be easily generalized to finite temperatures. Future works will focus on developing a density matrix approach in which permutational symmetries can be smoothly applied.

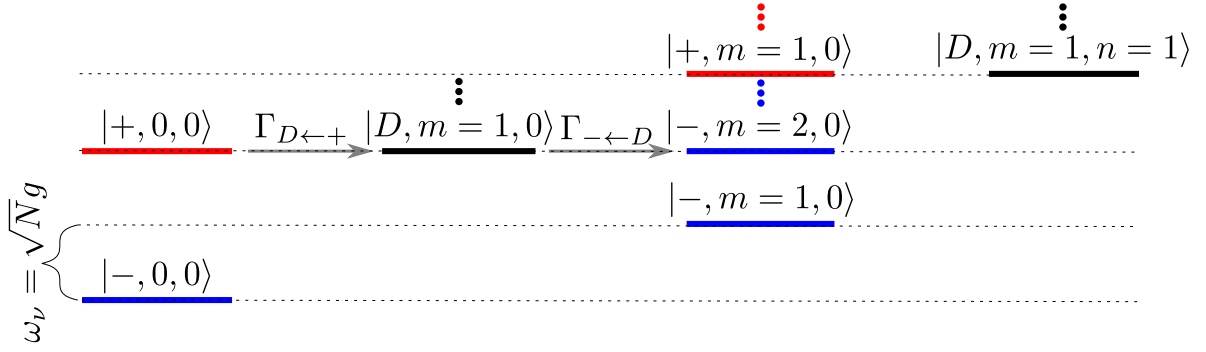


FIG. 5. Eigenstates of $\hat{H}_0^{(1)}$ and relaxation mechanism. States $|+, 0, 0\rangle$, $|D, m=1, 0\rangle$, and $|-, m=2, 0\rangle$ are resonantly coupled through vibronic coupling. $m=2$ means there are 2 phonons of frequency $\omega_\nu = \sqrt{N}g$ in the bath modes of the excited effective molecule. In the derivation, we have assumed the second phonon is emitted into a different bath mode than the first one.

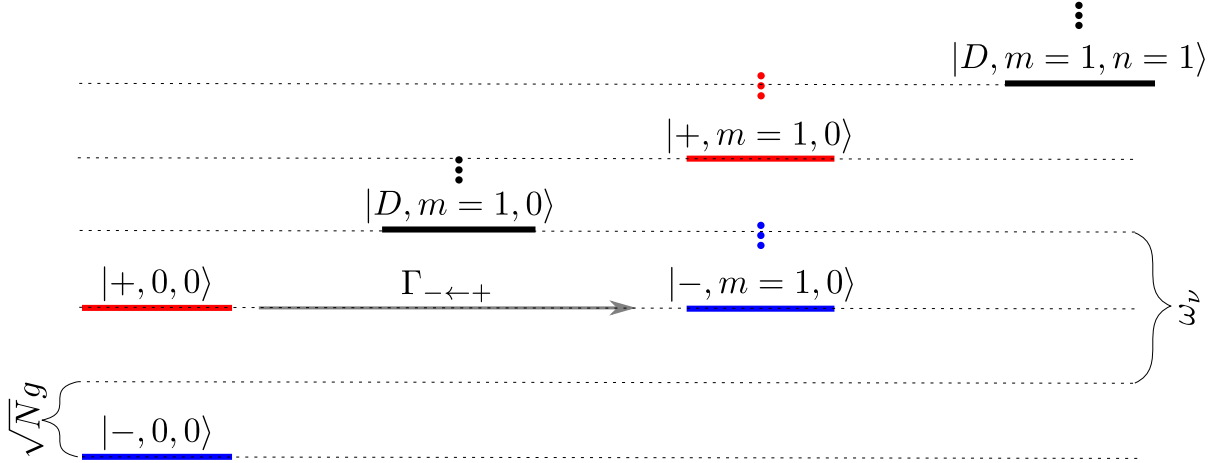


FIG. 6. Eigenstates of $\hat{H}_0^{(1)}$ and relaxation mechanism for $\omega_\nu = 2\sqrt{N}g$. States $|+, 0, 0\rangle$ and $|-, m=1, 0\rangle$ are resonantly coupled through vibronic coupling.

V. NON-STATISTICAL EXCITED STATE REACTIVITY

In this section, we look at the mechanism whereby, given two molecular species strongly coupled to a cavity, excitation energy can be selectively funneled to one of the species. We will show that statistical yield esti-

mates based on linear optical spectroscopy are inefficient at predicting these outcomes accurately.

For a system with N_A molecules of type A and N_B molecules of type B inside a cavity, the Hamiltonian in the zeroth-order approximation (see Eq. 15) can be readily generalized to,

$$\hat{H}_0 = \left(\begin{array}{c|ccc|ccc} \omega_c & g_A\sqrt{N_A}\langle\varphi_1^{(A)}|\phi_1^{(A)}\rangle & \cdots & g_A\sqrt{N_B}\langle\varphi_1^{(A)}|\phi_{m_A}^{(A)}\rangle & g_A\sqrt{N_A}\langle\varphi_1^{(B)}|\phi_1^{(B)}\rangle & \cdots & g_B\sqrt{N_B}\langle\varphi_1^{(B)}|\phi_{m_B}^{(B)}\rangle \\ \hline g_A\sqrt{N_A}\langle\varphi_1^{(A)}|\phi_1^{(A)}\rangle & \omega_{eg,1}^{(A)} & \cdots & 0 & 0 & \cdots & 0 \\ \vdots & 0 & \ddots & \vdots & \vdots & \ddots & \vdots \\ g_A\sqrt{N_A}\langle\varphi_1^{(A)}|\phi_{m_A}^{(A)}\rangle & \vdots & \cdots & \omega_{eg,m_A}^{(A)} & 0 & \cdots & 0 \\ \hline g_B\sqrt{N_B}\langle\varphi_1^{(B)}|\phi_1^{(B)}\rangle & 0 & \cdots & 0 & \omega_{eg,1}^{(B)} & \cdots & 0 \\ \vdots & \vdots & \ddots & \vdots & 0 & \ddots & \vdots \\ g_B\sqrt{N_B}\langle\varphi_1^{(B)}|\phi_{m_B}^{(B)}\rangle & 0 & \cdots & 0 & \vdots & \cdots & \omega_{eg,m_B}^{(B)} \end{array} \right) \quad (36)$$

The molecular PES in mass-weighted coordinates ($\mu = 1$) are $V_{g,j}(q_j) = \frac{1}{2}\omega_g^2 q_j^2$ where $j \in \{A, B\}$ denote the molecular species, $V_{e,A}(q_A) = \frac{1}{2}\omega_e^2(q_A - d_A)^2 + E_A$, and $V_{e,B}(q_B) = e^{-a(q_B - d_B)} + E_B$. For our simulations, we have chosen $\omega_g = \omega_e = 0.22$ eV, $d_A = d_B = 1.058$ Å, $a = 0.3$ Å⁻¹, $E_A = E_B = 2.2$ eV, and $g_A\sqrt{N_A} = g_B\sqrt{N_B} = 0.22$ eV. The photon energy (ω_c) is resonant with the FC transition of both A and B with $\omega_c = E_A + \frac{1}{2}\omega_e^2 d_A^2$ (see Fig. 7a).

To numerically construct \hat{H}_0 , we compute the eigenstates and eigen-energies of the vibrational Hamiltonians using the standard D.V.R method by Colbert and Miller [46]. This calculation was then used to compute spectra of the molecules outside and in the cavity using the formalism illustrated in [22, 31]. The spectra have been plotted in Fig. 7b. The absorption spectra of the bare molecules reveal the energy level structure about the FC regions [47]. For molecular species A , we see the strongest peak corresponding to the FC transition accompanied by the other peaks of the vibronic progression. On the other hand, for molecules of type B , we see a broad feature in the spectrum arising from the dense spectrum due to the dissociative potential. When strongly coupled with a cavity, these peaks form a rich pattern of peak splittings.

We build time-dependent wavefunctions by constructing the corresponding linear combinations of numerically computed eigenstates of $\hat{H}^{(0)}$. This simulation illustrates a phenomenon where the energy initially given to the cavity is eventually channeled preferentially to one of the two molecules. The results of this simulation are consistent with the phenomenology originally theoretically proposed by Groenhof and Toppari, based on computational simulations with at most 1000 molecules of a given species, [48], and demonstrate the latter remains valid in the thermodynamic limit. For our simulation, we start with an excitation in the cavity, $|\Psi(0)\rangle = \varphi_1(q_A)\varphi_1(q_B)|1\rangle$. At very short times the cavity distributes the energy into both types of molecules, exciting them at their respective FC regions. We monitor the excited state populations as a function of time (see Fig. 8a). We observe that at short times, the population is transferred equally to both species. However, as time progresses, the excitation is funneled selectively to species B via the cavity. The intuitive explanation of the

phenomenon is the following: at short times of the order of the Rabi oscillations, the cavity excites the bright modes of both molecules with equal populations at the respective FC regions due to the chosen equal collective light-matter couplings. However, as time progresses, excitations in molecules of type B decay irreversibly into the dark-states upon evolution away from the FC region (see Eq. 25) due to the dissociative character of the potential. Molecular species A does not undergo this irreversible dynamics due to the bound nature of its excited PESs. What results from this simulation is a net energy flow from molecular species A to species B mediated by the cavity, and which cannot be easily explained by the contribution of each molecule to the polariton states defined at the FC region [48].

Next, we map the populations accumulated in the excited states of molecules A and B to statistical estimates obtained from probabilities of molecules of each type being excited (p_{s_j} for $j \in \{A, B\}$) by the cavity:

$$p_{s_j} = \sum_n |\langle n|e_j\rangle|^2 |\langle n|1\rangle|^2 \quad (37)$$

Here, $\{|n\rangle\}$ represent the eigenstates of $\hat{H}^{(0)}$. Eq. 37 computes the composition of probabilities of an eigenstate simultaneously having photonic and molecule $A(B)$ contribution. However, the entire set of eigenstates is in practice not obtainable using linear absorption spectroscopy alone, given that the latter is a projection at the FC region [47]. As an extreme example, we consider adiabatic “low time resolution eigenstates” consisting of the upper, middle, and lower polaritons computed at the FC region. The statistical estimates obtained from this are represented as $p_{s_A}(FC)$ and $p_{s_B}(FC)$ in Fig. 8a. For the other case, we used the full set of eigenstates obtained through diagonalization of $\hat{H}^{(0)}$. The statistical estimates obtained using these are represented as p_{s_A} and p_{s_B} in Fig. 8a. The plot suggests that the statistical estimate obtained from the full set of eigenvectors gives the right prediction of the yields at long times, as expected. However, now the question arises, how much information of the full set of eigenstates is spectroscopically accessible, such that from a linear optical signal one can predict the yields to be expected from a photo-driven reaction? These questions become even more pertinent owing to some observations of Xiang *et al.* [10], where the authors observe selective cavity-mediated en-

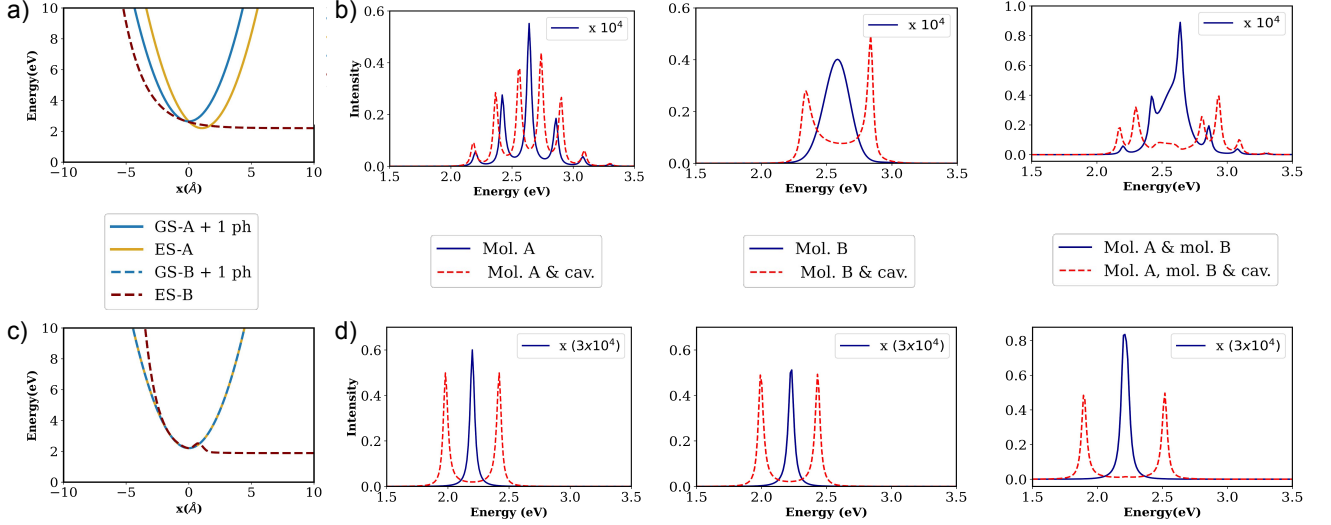


FIG. 7. a) Potential energy surfaces with (GS- $j+1$ ph) given as $V_{g,j}(q_j) = \frac{1}{2}\omega_g^2 q_j^2 + E_{ph}$, ES-A as $V_{e,A}(q_A) = \frac{1}{2}\omega_e^2 (q_A - d_A)^2 + E_A$ and ES-B as $V_{e,B}(q_B) = e^{-a(q_B - d_B)} + E_B$ with $\omega_g = \omega_e = 0.22$ eV, $d_A = d_B = 1.058$ Å, $a = 0.3$ Å⁻¹, $E_A = E_B = 2.2$ eV and photon energy (E_{ph}) = $E_A + \frac{1}{2}\omega_e^2 d_A^2$, b) Absorption spectra of the molecules outside and inside the cavity for a, c) Potential energy surfaces with GS- j same as a), ES-A same as a) with $d_A = 0$ and, ES-B as $V_{e,B}(q_B) = e^{-a(q_B - d_{B,1})} + c \cdot e^{-b(q_B - d_{B,2})^2} + E_B$. The parameters used are $a = 0.51$ Å⁻¹, $d_{B,1} = 0.26$ Å, $b = 1.2$ Å⁻², $c = 2.3$ eV and $d_{B,2} = 0.79$ Å and $E_B = 1.88$ eV, d) Absorption spectra of the molecules outside and inside the cavity for c. For a and c, the x -axis is q_1 for molecular species 1 and q_2 for molecular species 2.

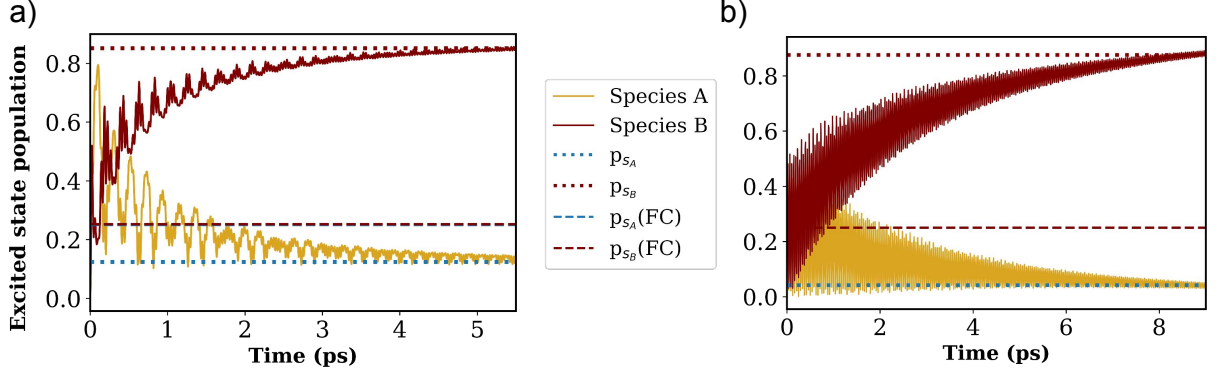


FIG. 8. The populations in the excited states of molecules of type A and B plotted as a function of time. The dashed lines show the estimated statistical populations from the polaritonic eigenstates at the FC point ($p_{s_A}(FC)$ and $p_{s_B}(FC)$). The dotted line shows the estimated populations from the entire set of eigenstates of the system (p_{s_A} and p_{s_B}) in: a) For the dissociative excited state, b) For the dissociative potential with bump.

ergy transfer into one of two molecules, despite the bare linear absorption spectral lineshapes being very similar outside the cavity.

Inspired by this question, we explore a slightly different shapes of the excited state PES for molecular species B such that it resembles that of molecular species A in the FC region. We now have $V_{e,B}(q_B) = e^{-a(q_B - d_{B,1})} + c e^{-b(q_B - d_{B,2})^2} + E_B$ as the excited state potential of molecular species B. Otherwise, the parameters are $\omega_g = \omega_e = 0.22$ eV, $d_A = 0$, $a = 0.51$ Å⁻¹, $d_{B,1} = 0.26$ Å, $b = 1.2$ Å⁻², $c = 2.3$ eV and $d_{B,2} = 0.79$ Å, and

$E_B = 1.88$ eV. The shapes of the PESs for this case are shown in Fig. 7c.

The computed spectra for both bare molecules under strong coupling to the cavity mode are shown in Fig. 7d. The resemblance of the excited state PESs of the two molecular species at the FC region translates into very similar spectral lineshapes for the bare molecules and when coupled to the cavity, confirming that linear spectroscopy can only efficiently probe projections of eigenstates at the FC region. The dissociative *vs* bound nature of the PESs away from the FC region is not efficiently

captured in these spectra, because from a time-dependent perspective, the dissociative potential contributes minimally to the lineshape through slow tunneling from the bound potential of the FC region.

Starting the dynamics with an excitation in the cavity mode, we see that, just like in the previous example, at short timescales, the cavity distributes the energy democratically to both species. The distribution of populations remains this way until the excitation in molecular species B tunnels through the barrier to decay into the dark states away from the FC region. That gives an analogous trend as in the previous case. We now need to compare the dynamical behavior to statistical predictions of the yield.

Since the spectra only efficiently capture information about the FC region, which is similar for the two species, the statistical ratio computed from the eigenstates at the FC point would predict equal populations of molecular species A and B. Thus the statistical estimate from linear spectroscopy does not fully capture the long time dynamics of the system due to its emphasis on the FC region. However, the theoretical estimates from the full set of eigenstates of the system (p_{s_A} and p_{s_B} in Fig.8b), which are hard to obtain from linear spectroscopy, can predict correct yields at long times originating from dynamics away from the FC region.

VI. SUMMARY

In this work we have developed a formalism that exploits permutational symmetries of an arbitrary number of identical molecules confined to an optical microcavity to elucidate their excited state dynamics under collective strong light-matter interaction. Although previous works have used equivalent symmetry arguments and have arrived at conclusions that are consistent with ours [22, 23, 31, 41, 49], elements of the present work uniquely provide opportunities for a systematic and intuitive treatment of molecular polariton dynamics. It is important to note that, although via quite a different formalism,

another method that maps the dynamics of molecular polaritons to a single effective molecule in a cavity has already recently been reported before our work [22]. This method, however, is based on density matrices and does not provide $\mathcal{O}(1/\sqrt{N})$ corrections to dynamics, and considers a coherent state of the photon at all times, instead of the single-excitation manifold dynamics we have presented. We believe this method is quite complementary in its scope to ours. However, given the different formalisms, it is at present hard to assess the deeper conceptual connections between the methods; this will be subject of future work.

Let us highlight some of the features of our approach. First, it allows for the systematical introduction of corrections to the thermodynamic limit. Second, our time-dependent approach generalizes some of the results found in previous work that also exploit permutational symmetries to compute optical properties; here we have generalized these concepts to chemical dynamics. Moreover, our work naturally provides an alternative interpretation of bright and dark-states based on permutationally-symmetric states, that is different from the one inherited from restrictive quantum optics models. These observations provide much needed physical intuition to design principles of polariton chemistry control, where rather than avoiding the decay into dark states, one embraces such phenomenon at one's advantage, such as with the examples provided in section V. Finally, the method enjoys numerical simplicity and is written in a language that makes it ideal for implementation in existing quantum and classical molecular dynamics algorithms.

VII. ACKNOWLEDGMENTS

This work was supported as part of the Center for Molecular Quantum Transduction (CMQT), an Energy Frontier Research Center funded by the U.S. Department of Energy, Office of Science, Basic Energy Sciences under Award No. DE-SC0021314. We also thank Kai Schwenicke and Matthew Du for useful discussions.

-
- [1] J. A. Hutchison, T. Schwartz, C. Genet, E. Devaux, and T. W. Ebbesen, *Angewandte Chemie International Edition* **51**, 1592 (2012).
 - [2] F. Herrera and J. Owrutsky, *The Journal of Chemical Physics* **152**, 100902 (2020).
 - [3] S. Pannir-Sivajothi, J. A. Campos-Gonzalez-Angulo, L. A. Martínez-Martínez, S. Sinha, and J. Yuen-Zhou, *Nature Communications* **13**, 1645 (2022).
 - [4] R. F. Ribeiro, L. A. Martínez-Martínez, M. Du, J. Campos-Gonzalez-Angulo, and J. Yuen-Zhou, *Chem. Sci.* **9**, 6325 (2018).
 - [5] A. Mandal and P. Huo, *The Journal of Physical Chemistry Letters* **10**, 5519 (2019), pMID: 31475529.
 - [6] R. H. Tichauer, J. Feist, and G. Groenhof, *The Journal of Chemical Physics* **154**, 104112 (2021).
 - [7] M. Reitz, F. Mineo, and C. Genes, *Scientific Reports* **8**, 9050 (2018).
 - [8] C. A. DelPo, S.-U.-Z. Khan, K. H. Park, B. Kudisch, B. P. Rand, and G. D. Scholes, *The Journal of Physical Chemistry Letters* **12**, 9774 (2021), pMID: 34595929.
 - [9] X. Zhong, T. Chervy, S. Wang, J. George, A. Thomas, J. A. Hutchison, E. Devaux, C. Genet, and T. W. Ebbesen, *Angewandte Chemie International Edition* **55**, 6202 (2016).
 - [10] B. Xiang, R. F. Ribeiro, M. Du, L. Chen, Z. Yang, J. Wang, J. Yuen-Zhou, and W. Xiong, *Science* **368**, 665 (2020).
 - [11] L. A. Martínez-Martínez, R. F. Ribeiro, J. Campos-González-Angulo, and J. Yuen-Zhou, *ACS Photonics* **5**, 167 (2018).

- [12] T. Ishii, F. Bencheikh, S. Forget, S. Chénais, B. Heinrich, D. Kreher, L. Sosa Vargas, K. Miyata, K. Onda, T. Fujihara, S. Kéna-Cohen, F. Mathevet, and C. Adachi, *Advanced Optical Materials* **9**, 2101048 (2021).
- [13] C. R. Gubbin, S. A. Maier, and S. Kéna-Cohen, *Applied Physics Letters* **104**, 233302 (2014).
- [14] T. Ishii, K. Miyata, M. Mamada, F. Bencheikh, F. Mathevet, K. Onda, S. Kéna-Cohen, and C. Adachi, *Advanced Optical Materials* **10**, 2102034 (2022).
- [15] S. Kéna-Cohen and S. R. Forrest, *Nature Photonics* **4**, 371 (2010).
- [16] M. Tavis and F. W. Cummings, *Phys. Rev.* **170**, 379 (1968).
- [17] J. M. Fink, R. Bianchetti, M. Baur, M. Göppl, L. Steffen, S. Filipp, P. J. Leek, A. Blais, and A. Wallraff, *Phys. Rev. Lett.* **103**, 083601 (2009).
- [18] I. Carusotto and C. Ciuti, *Rev. Mod. Phys.* **85**, 299 (2013).
- [19] J. del Pino, F. A. Y. N. Schröder, A. W. Chin, J. Feist, and F. J. Garcia-Vidal, *Phys. Rev. Lett.* **121**, 227401 (2018).
- [20] F. Herrera and F. C. Spano, *Phys. Rev. Lett.* **118**, 223601 (2017).
- [21] G. Groenhof, C. Climent, J. Feist, D. Morozov, and J. J. Toppari, *The Journal of Physical Chemistry Letters* **10**, 5476 (2019), pMID: 31453696.
- [22] P. Fowler-Wright, B. W. Lovett, and J. Keeling, *Efficient many-body non-markovian dynamics of organic polaritons* (2021).
- [23] F. C. Spano, *The Journal of Chemical Physics* **152**, 204113 (2020).
- [24] F. C. Spano, *The Journal of Chemical Physics* **142**, 184707 (2015).
- [25] N. Shammah, S. Ahmed, N. Lambert, S. De Liberato, and F. Nori, *Phys. Rev. A* **98**, 063815 (2018).
- [26] F. Herrera and F. C. Spano, *ACS Photonics* **5**, 65 (2018).
- [27] R. E. F. Silva and J. Feist, *Phys. Rev. A* **105**, 043704 (2022).
- [28] M. A. Zeb, *Computer Physics Communications* **276**, 108347 (2022).
- [29] J. A. Campos-Gonzalez-Angulo and J. Yuen-Zhou, *The Journal of Chemical Physics* **156**, 194308 (2022).
- [30] L. S. Cederbaum, *The Journal of Chemical Physics* **156**, 184102 (2022).
- [31] M. A. Zeb, P. G. Kirton, and J. Keeling, *ACS Photonics* **5**, 249 (2018).
- [32] J. A. Ćwik, P. Kirton, S. De Liberato, and J. Keeling, *Phys. Rev. A* **93**, 033840 (2016).
- [33] G. J. Halász, M. Šindelka, N. Moiseyev, L. S. Cederbaum, and g. Vibók, *The Journal of Physical Chemistry A* **116**, 2636 (2012), pMID: 22043872.
- [34] O. Vendrell, *Physical Review Letters* **121**, 10.1103/physrevlett.121.253001 (2018).
- [35] G. A. Worth, M. H. Beck, A. Jäckle, and H.-D. Meyer, *The MCTDH Package, Version 8.2* (2000).
- [36] F. C. Spano and H. Yamagata, *The Journal of Physical Chemistry B* **115**, 5133 (2011), pMID: 20957993.
- [37] N. Makri, *The Journal of Physical Chemistry B* **103**, 2823 (1999).
- [38] M. Schubert, *Phys. Rev. B* **53**, 4265 (1996).
- [39] V. M. Agranovich, M. Litinskaia, and D. G. Lidzey, *Phys. Rev. B* **67**, 085311 (2003).
- [40] I. S. Ulusoy, J. A. Gomez, and O. Vendrell, *The Journal of Physical Chemistry A* **123**, 8832 (2019), pMID: 31536346.
- [41] B. Cui and A. Nitzan, *Collective response in light-matter interactions: The interplay between strong coupling and local dynamics* (2022).
- [42] R. F. Ribeiro, L. A. Martínez-Martínez, M. Du, J. Campos-Gonzalez-Angulo, and J. Yuen-Zhou, *Chem. Sci.* **9**, 6325 (2018).
- [43] J. del Pino, J. Feist, and F. J. Garcia-Vidal, *New Journal of Physics* **17**, 053040 (2015).
- [44] M. Litinskaya, P. Reineker, and V. Agranovich, *Journal of Luminescence* **110**, 364 (2004), 325th Wilhelm and Else Heraeus Workshop. Organic Molecular Solids : Excited Electronic States and Optical Properties.
- [45] B. Munkhbat, M. Wersäll, D. G. Baranov, T. J. Antosiewicz, and T. Shegai, *Science Advances* **4**, eaas9552 (2018).
- [46] D. T. Colbert and W. H. Miller, *The Journal of Chemical Physics* **96**, 1982 (1992).
- [47] E. J. Heller, *Accounts of Chemical Research* **14**, 368 (1981).
- [48] G. Groenhof and J. J. Toppari, *J. Phys. Chem. Lett.* **9**, 4848 (2018).
- [49] C. Schäfer, *The Journal of Physical Chemistry Letters* **13**, 6905 (2022).